[30] D. Winkelmann, Z. Elektrochem. **60**, 731 [1956].
[31] F. Haber, Z. anorg. Allg. Chem. **51**, 356 [1906].
[32] L. Müller u. L. N. Nekrassow, J. Electroanal. Chem. **9**, 282 [1965].
[33] M. A. Genshaw, A. Damjanowitsch u. J. O'M. Bockris, J. Electrochem. Soc. **15**, 163, 173 [1967].
[34] B. Kastening u. G. Kazemifard, Ber. Bunsenges. Physik. Chem. **74**, 551 [1970].
[35] W. G. Berl, Transact. Electrochem. Soc. **83**, 253 [1943].
[36] F. Haber u. J. Weiss, Proc. Roy. Soc. London Ser. A **147**, 332 [1934].
[37] J. Weiss, Trans. Faraday Soc. **31**, 1547 [1935], vgl. Adv. Catalysis **4**, 343 [1952].
[38] V. S. Bagotskii, L. N. Nekrassow u. N. A. Schumilowa, Russ. Chem. Rev. **34**, 717 [1965].
[39] R. Gerischer u. H. Gerischer, Z. Physik. Chem. (N.F.) **6**, 178 [1956].
[40] F. Beck, Ber. Bunsenges. Physik. Chem. **77**, 353 [1973].
[41] L. D. Rollmann u. R. T. Iwamoto, J. Amer. Chem. Soc. **90**, 1455 [1968].
[42] J. Manassen u. A. Bar-Ilan, J. Catalysis **17**, 86 [1970].
[43] A. E. Martell u. M. Calvin, Die Chemie der Metallchelate, Verlag Chemie, Weinheim 1958.
[44] A. Sigel, Angew. Chem. **81**, 161 [1969].
[45] H. Alt, H. Binder, A. Köhling u. G. Sandstede, Electrochim. Acta **17**, 873 [1972].

Photoreactions of Small Organic Molecules

I. Mass-Spectrometric Study of Vinylchloride, Vinylfluoride and 1,1-Difluoroethylene in the Vacuum Ultraviolet

D. Reinke, R. Kraessig, and H. Baumgärtel

Institut für Physikalische Chemie der Universität Freiburg i. Br.

(Z. Naturforsch. **28 a**, 1021–1031 [1973]; received 10 February 1973)

The photoionization curves and the threshold energies for the molecules vinylchloride, vinylfluoride, 1,1-difluoroethylene and their abundant fragment ions have been measured with synchrotron radiation in the photon energy range from 10–23 eV. Appearance potentials were used to calculate heats of formation, bond energies and ionization potentials. The structure of ion efficiency curves is discussed in terms of different ionization processes.

Introduction

Photoelectron spectroscopy using resonance line radiation is a convenient technique for investigating the energy of atomic and molecular orbitals [1, 2]. To excite valence levels of organic molecules, the He(I) (21.21 eV) line is generally used. The energy of photoelectrons gives evidence of direct transitions into the ionization continuum. If an experiment with variable excitation energy and mass analysis is performed, the appearance potentials of photofragmentation and photoionization processes are observable [3–5].

From the appearance potentials, heats of formation of the ions and radicals involved in the photoreaction may be calculated and bond-dissociation and ionization energies obtained.

To get information about the same fragments as they emerge from different molecules, we have studied vinylchloride, vinylfluoride and 1,1-difluoroethylene. Fluoroethylenes were the subject of several investigations using electron impact with mass analysis [6–8]. Experiments using photoionization techniques in mass spectrometry have shown that the results of electron impact experiments are often questionable.

Since LiF windows were used, earlier work on photoionization of halogen derivatives of ethylene was restricted to wavelengths greater than about 1040 Å [9, 6]. In the present work we will represent photoionization efficiency curves of parent ions and their fragments from the onset region up to about 23 eV. The experimental arrangement comprises an electron-synchrotron as light source, an vacuum-ultraviolet monochromator and a quadrupole mass analyzer.

Experimental Setup *

The characteristics of the continuous spectrum emitted by the 7.5 GeV electron accelerator DESY have been described in the literature [10]. The light is emitted tangentially from the electron orbit. Over a distance of about 40 m towards the monochromator the light is reflected twice (angle of incidence 83°)

Reprint requests to Dr. H. Baumgärtel, Institut für Physikalische Chemie der Universität Freiburg, *D-7800 Freiburg*, Albertstraße 21.

* The experiments were performed at the Deutsches Elektronen-Synchrotron DESY, Hamburg.

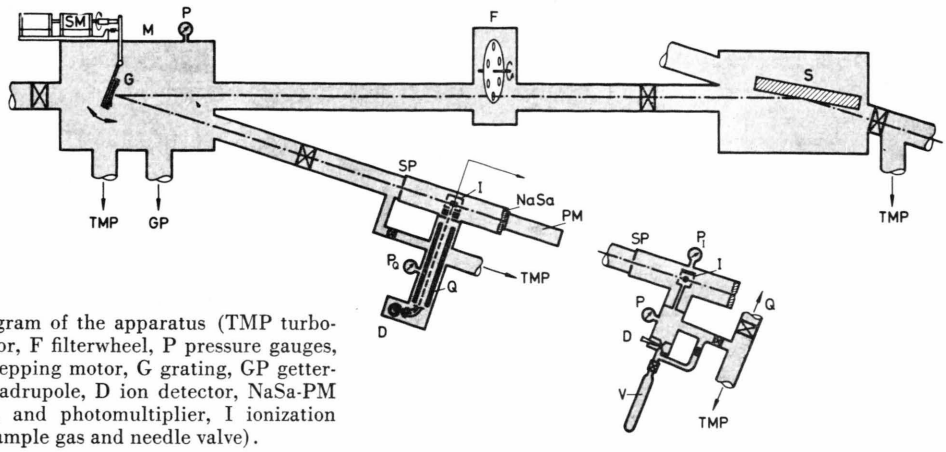

Fig. 1. Schematic of diagram of the apparatus (TMP turbomolecular pumps, S mirror, F filterwheel, P pressure gauges, M monochromator, SM stepping motor, G grating, GP getterpump, SP exit slit, Q quadrupole, D ion detector, NaSa-PM sodium salicylate screen and photomultiplier, I ionization chamber, V, D, sample gas and needle valve).

with the plane of incidence lying perpendicular to the synchrotron plane.

The monochromator operates in a modified Wadsworth mounting [11, 12] with the dispersion plane perpendicular to the synchrotron plane (Figure 1). This results in an optimal resolution of 0.7 Å limited by the dimension of the light source image at the exit slit. A gold coated 1200 lines/mm Bausch & Lomb grating blazed at 600 Å and 1 m focal length was used, yielding a linear dispersion of 7.5 Å/mm.

The light transmitted through the ionization chamber was measured by counting the photons emitted from a sodium salicylate screen with a photomultiplier (EMI 9502 S). The fluorescence yield of sodium salicylate is nearly independent of the energy of the exciting radiation between 10 – 25 eV [13]. The first order spectrum detected with this arrangement is shown in Figure 2. The contributions of second order radiation were estimated from absorption edge measurements with indium and antimony filters in the first and second order. It amounts to about 0.4% at 800 Å and 15% at 1500 Å and, together with the scattered light, contributes a wavelength dependent background ion current which was not corrected for.

The photon wavelength was varied by a stepping motor remotely controlled by a preset indexer, one step being 0.27 Å. The energy calibration was determined to be correct within ±1.5 Å by taking the photoionization spectra of O_2, N_2 and some rare gases.

Behind the monochromator exit slit the photon beam traverses the ionization chamber which is 30 mm in width. The ions produced there are extracted by a repeller and focused onto the 3 mm ϕ entrance aperture of the quadrupole mass spectrometer (Balzers QMG 101) with an electrostatic single lens system. The electrostatic potentials were adjusted to get maximum ion efficiency without impairing the mass resolution. The mass analyzed ions were detected by an channeltron multiplier (Bendix 4028) and counting system (SEN 300), 10 – 500 counts/sec being representative of normal operating conditions.

Sample gases were introduced into the ionization chamber at pressures not higher than about 10^{-4} Torr. The pressure was monitored by a precision membrane-vacummeter (Datametrix).

No correction was made for a long time pressure decrease of about 10%. The ionization chamber housing is separated from the monochromator and the quadrupole by a differential pumping system. With two turbomolecular pumps (Pfeiffer TVP 250/500) a pressure of about $10^{-5} - 10^{-6}$ Torr can be maintained outside the ion source housing under operating conditions. Further details of the experimental arrangement and the electronics are given in References [14, 15].

Fig. 2. First order spectra of the monochromator with gold coated gratings (1200 lines/mm, 600 Å blaze). (1) grating 1, new; (2) grating 1, 16 months in use; (3) grating 2, new. The intensities of the three spectra are normalized at the maximum.

Fig. 3. Ionization efficiency for $C_2H_3Cl^+$, $C_2H_3^+$ and $C_2H_2^+$ from C_2H_3Cl. The cross sections are relative to one another. The arrows indicate ionization potentials taken from Ref. [17].

Fig. 4. Ionization efficiency for $C_2H_3F^+(46)$, $C_2H_2F^+(45)$, $C_2HF^+(44)$, $C_2H_3^+(27)$ and $C_2H_2^+(26)$ from C_2H_3F.

Fig. 5. Ionization efficiency for $C_2H_2F_2^+(64)$, $C_2HF_2^+(63)$, $C_2H_2F^+(45)$, $C_2HF^+(44)$, $CH_2F^+(33)$, $CF^+(31)$, $C_2H_2^+(26)$ and $CH_2^+(14)$ from $C_2H_2F_2$.

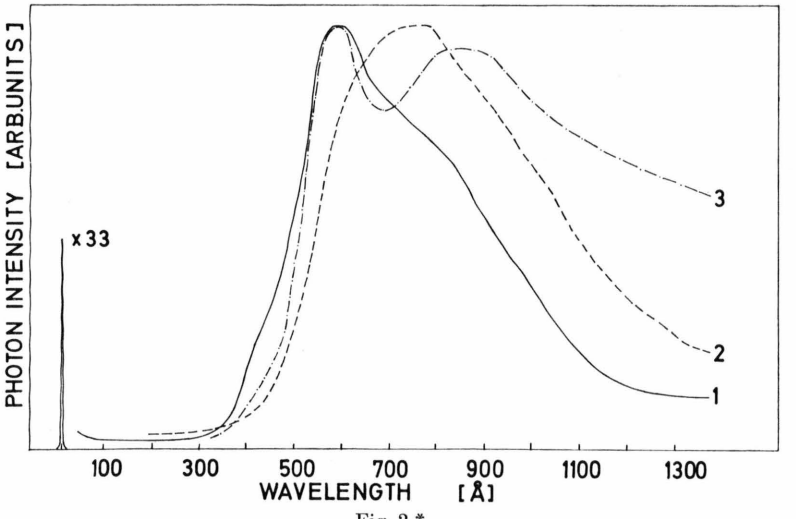

Fig. 2 *.

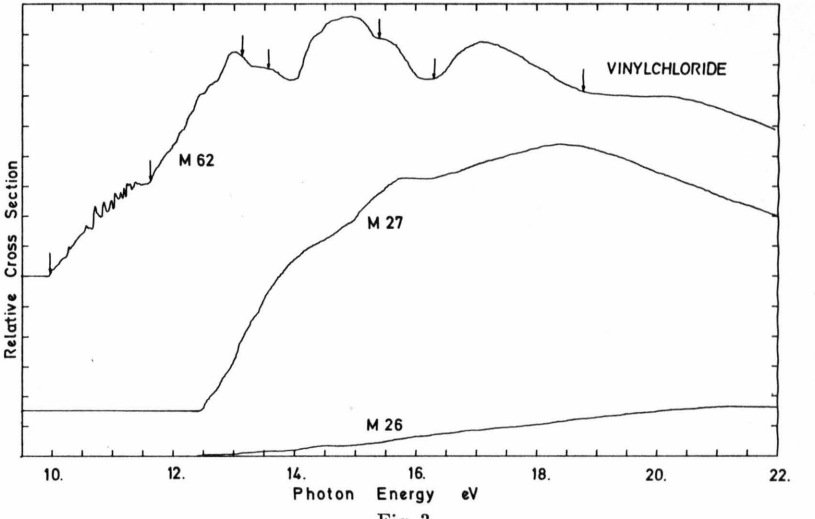

Fig. 3.

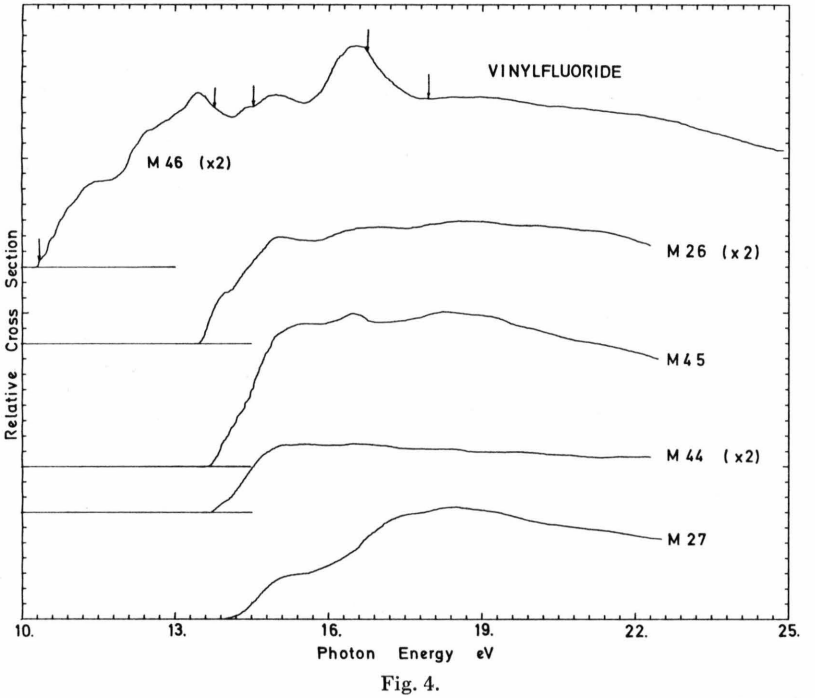

Fig. 4.

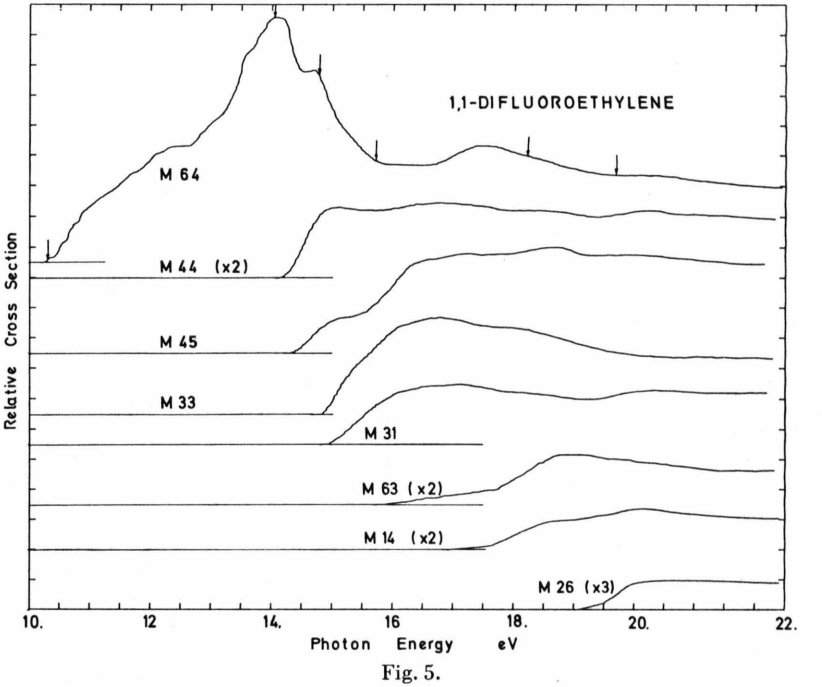

Fig. 5.

* The legends of Figs. 2—5 stand at the bottom of page 1022.

With the help of the known absolute photoionization cross sections of Ne, Ar, Kr, and Xe [13] an estimate of both the photon intensity behind the exit slit of the monochromator and the mass transmission function of the quadrupole was obtained.

With 30 mA electron current in the synchrotron we get about 10^7 photons sec^{-1} $Å^{-1}$ at 600 Å. Using a resolution sufficient to separate adjacent masses clearly the transmission for different masses was determined to lie between about 60% (mass 20) and 25% (mass 84). The transmission of masses occuring in our investigation is estimated to be within the limits 40 – 70%.

Results

Figures 3 – 5 show the relative cross sections for production of the vinylchloride, vinylfluoride and 1,1 difluorethylene parent and fragment ions as functions of the photon energy.

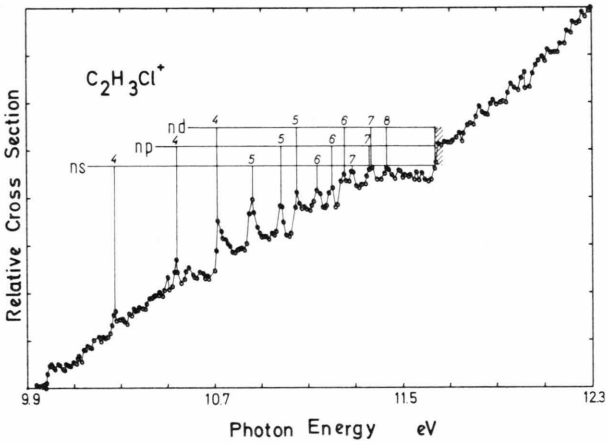

Fig. 6. Onset region of $C_2H_3Cl^+$ efficiency curve.

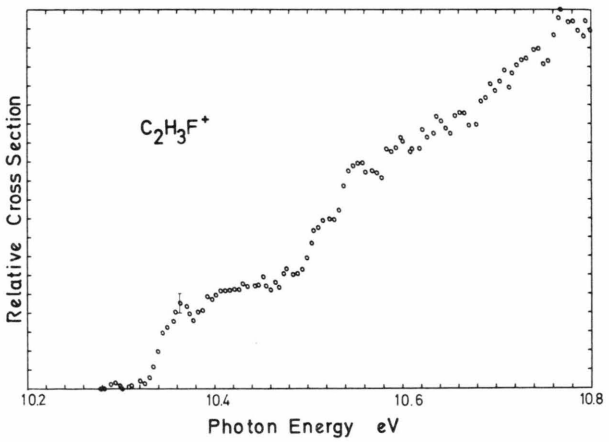

Fig. 7. Onset region of $C_2H_3F^+$ efficiency curve.

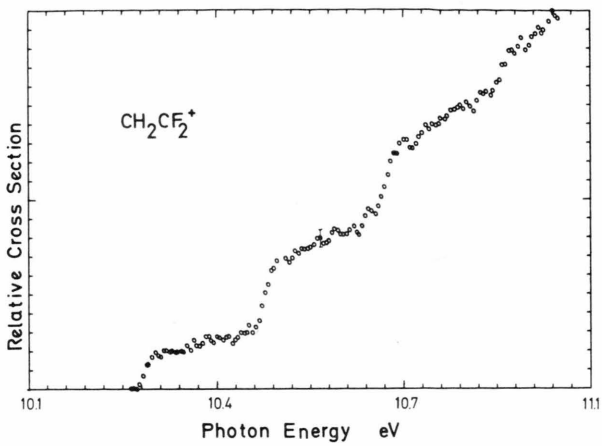

Fig. 8. Onset region of $C_2H_2F_2^+$ efficiency curve.

The curves represent the result of a graphical smoothing procedure containing the digital data of several runs. The statistical error in the ion counting is about equal to four times the size of the points in Fig. 7 and 8. In Table 1, results from all ions are summarized together with their appearance potentials and their relative intensity related to the total ion efficiency at 550 Å. The mass intensities are not corrected for the slightly mass dependent transmission of our quadrupole. For the parent ions the first step in the efficiency curve is deconvoluted with the monochromator slit function to get the appearance potential. All data were taken with 150 μ exit slits yielding about 1.2 Å resolution. Most fragment-ion thresholds are taken as the point of intersection with the background count. The gases were research grade materials obtained from Matheson Company. In their mass spectra, no impurities of significance for this study were detected.

Discussion

1. Appearance Potentials and Fragment Ion Efficiencies

When one of the higher molecular orbitals of a molecule is ionized a radicalcation remains, containing internal excitation energy $E^* = I - I_0$, where I_0 is the lowest ionization potential of the molecule.

In an isolated ion this excitation energy can be lost by radiative or dissociation processes. In the latter case some of the energy is used in bond breaking, the rest appearing as kinetic energy or internal excitation of the products.

Table 1. Appearance potentials of C_2H_3Cl, C_2H_3F and 1,1-CH_2CF_2 compared with electron impact values * from References [6, 7].

Ion	Mass	*AP* (eV) this work	*AP* (eV)*	Rel. Efficiency %) at 22.5 eV
$C_2H_3Cl^+$	62	9.99 ± 0.01	10.10 / —	37
$C_2H_3^+$	27	12.48 ± 0.04	13.00 / —	50
$C_2H_2^+$	26	12.47 ± 0.1	— / —	13
$C_2H_3F^+$	46	10.35 ± 0.01	— / 10.45	22
$C_2H_2F^+$	45	13.56 ± 0.04	14.10 / 14.02	31
C_2HF^+	44	13.72 ± 0.02	14.10 / 14.04	8
$C_2H_3^+$	27	13.84 ± 0.04	14.47 / 14.38	24
$C_2H_2^+$	26	13.51 ± 0.02	— / 13.73	15
$C_2H_2F_2^+$	64	10.29 ± 0.01	10.32 / 10.45	22
$C_2HF_2^+$	63	15.80 ± 0.04	— / 16.67	5
$C_2H_2F^+_2$	45	14.37 ± 0.02	14.80 / 14.80	25
C_2HF^+	44	14.18 ± 0.03	14.42 / 14.44	9
CH_2F^+	33	14.84 ± 0.02	15.28 / 15.08	17
CF^+	31	14.92 ± 0.02	15.16 / 15.23	15
$C_2H_3^+$	26	19.08 ± 0.03	— / 19.78	2
CH_2^+	14	16.99 ± 0.02	— / 17.8	5

For the photoreaction

$$AB + h\nu \rightarrow A^+ + B + e,$$

the following relationship holds:

$$AP(A^+) = \Delta H_f(A^+) + \Delta H_f(B) - \Delta H_f(AB) + E$$
$$= D(A-B) + IP(A) + E,$$

with $AP(A^+)$: Appearance potential of ion A^+

$\Delta H_f(A^+, B, AB)$: standard heat of formation of A^+, B, AB,

$D(A-B)$: dissociation energy of bond A – B,

$IP(A)$: ionization potential of fragment A.

Without a further investigation of the fragments, one is not able to determine the character of the excess energy term E either in our and other photoionization experiments. In the immediate future, our experimental arrangement will be changed to permit the detection of fluorescent excited states too. Nevertheless, photoionization thresholds permit an accurate determination of a number of thermochemical quantities since many mass spectrometric fragmentation processes do not involve excess energy. This problem is discussed in detail in section Ia – Ic for the compounds investigated. It is possible to propose in most cases fragmentation mechanisms based only on energetic considerations. The following discussion treats the energetic aspect of the data in Table 1 with respect to the thermodynamic relation cited above. Where not otherwise quoted the energies of formation used are taken from reference [16]. All data refer to 298 °K. The corrections to be made for 0 °K data taken from the literature are mostly within the error limits of the enthalpy data.

Ia. Vinylchloride

The minimum energy for the onset of ionization occurs at 9.99 ± 0.02 eV in good agreement with the photoelectron-spectroscopic value of 10.00 eV for the adiabatic ionization potential [17].

Beyond the second ionization potential two fragmentation processes begin, one resulting in the elimination of the chlorine atom via

$$C_2H_3Cl + h\nu = C_2H_3^+ + Cl + e. \qquad (1)$$

The thermodynamic energy equation applied to (1) yields

$$AP(C_2H_3^+) = \Delta H_f(C_2H_3^+) + \Delta H_f(Cl) - \Delta H_f(C_2H_3Cl) + E = D(C_2H_3 - Cl) + IP(C_2H_3) + E.$$

From the reaction

$$C_2H_4 + h\nu \rightarrow C_2H_3^+ + H + e \qquad (2)$$

measured by Berkowitz, Chupka and Rafaey [18], we find $\Delta H_f(C_2H_3^+)$ to be 265 ± 2 kcal/mole. The values $\Delta H_f(C_2H_3Cl) = 5.2$ kcal/mole and $\Delta H_f(Cl) = 28.9$ kcal/mole are quoted in the literature [19, 16]. From the energetic relation corresponding to reaction (1) and our $AP(C_2H_3^+)$ we obtain $H_f(C_2H_3^+) = 264 \pm 2$ kcal/mole. From the close agreement of these values we conclude that excess energy is probably not involved.

The pair formation process $C_2H_3Cl + h\nu \rightarrow C_2H_3^+ + Cl^-$ should start about 3,6 eV lower and could not be detected.

With the confirmed value of $\Delta H_f(C_2H_3^+)$ and the known heat of formation of C_2H_3, $\Delta H_f(C_2H_3) = 64$ kcal/mole [21], we find $IP(C_2H_3) = \Delta H_f(C_2H_3^+) - \Delta H_f(C_2H_3) = 8.7 \pm 0.1$ eV for the ionization potential of the vinylradical. Beck [20] reports a directly determined electron impact value of 9.4 ± 0.2 eV which seems to be too high. If the ionization potential of the C_2H_3 radical is taken to be 8.7 eV, we are also able to recalculate the dissociation energy $D(C_2H_3 - Cl) = 89$ kcal/mole given in Reference [18]. With the aid of reaction (2) and the $AP(C_2H_3^+) = 13.19$ eV mentioned there, we arrive at $D(C_2H_3 - H) = 104 \pm 2$ kcal/mole. A compilation of different values by Kerr [21] yielded the same value of $C_2H_3^+$ taken in process (1), we get the bond dissociation energy $D(C_2H_3 - Cl) = 87 \pm 2$ kcal/mole.

A comparison of Fig. 3 and the photoelectron spectrum of Lake and Thompson [17] indicates that the fragmentation process may not take place in the aforementioned (Section I) way with the ionization as the primary step. Both fragmentations in C_2H_3Cl start between the second and the third ionization potential where no population of an excited stationary ion state can be seen in the photoelectron spectrum. Transitions to a repulsive ion state are unlikely to occur due to the absence of a marked continuum of photoelectrons in this region [17]. As we further exclude a pair formation process, we have to assume that a neutral molecular state is reached which autoionizes into an ion state with sufficient internal energy to decay.

As described in Section II, we expect an excited state to lie in this region. This assumption is given further support by the strong increase of the ionization cross section beyond the second ionization potential, whereas one would expect a flat region if only direct ionization were present.

We see no difference between $AP(C_2H_3^+)$ and the appearance potential of the $C_2H_2^+$ ion. The onset of the second ion has a long tail which makes it difficult to estimate an accurate appearance potential for the reaction:

$$C_2H_3Cl + h\nu \rightarrow C_2H_2^+ + HCl + e\,. \qquad (3)$$

The $AP(C_2H_2^+)$ determined in this HCl elimination process yields the heat of formation of $C_2H_2^+$ as $\Delta H_f(C_2H_2^+) = 315 \pm 4$ kcal/mole. Within the error limits this value agrees with $\Delta H_f(C_2H_2^+) = 317.2$ kcal determined from

$$H_f(C_2H_2^+) = \Delta H_f(C_2H_2) + IP(C_2H_2) = 54.2 + 263.1 \text{ kcal/mole}\,[16, 22] = 317 \text{ kcal/mole} \qquad (4)$$

with the $IP(C_2H_2)$ from the photoionization of C_2H_2.

We therefore conclude that (3) describes the formation of the acetylene structure of $HCCH^+$, the H and the Cl atom in the unimolecular transition state being from neighbouring carbon atoms.

At 550 Å we also detected the fragments $C_2H_2Cl^+$ and C_2HCl^+ with an intensity considerably lower than that of the measured ions.

Ib. Vinylfluoride

The ionization potential of vinylfluoride was determined to be $IP(C_2H_3F) = 10.35 \pm 0.01$ eV, a value somewhat lower than the photoelectronspectroscopic result of 10.37 eV [17]. At higher photon energies we observed four fragmentation processes. In contrast to C_2H_3Cl, the elimination of a hydrogen atom together with the fluorine loss is the most intense decomposition process:

$$C_2H_3F + h\nu \rightarrow C_2H_2F^+ + H + e\,. \qquad (5)$$

A comparison with other saturated and unsaturated hydrocarbons [4, 18] indicates that the frequency factor for breaking the C – H bond is considerably larger, presumably due to particular bonding properties of the hydrogen within the CHF group. With

$$\Delta H_f(C_2H_3F) = -28 \text{ kcal/mole}\,[23] \quad \text{and}$$
$$\Delta H_f(CH_2CF^+) = AP(CH_2CF^+) - \Delta H_f(H) + \Delta H_f(C_2H_3F)$$

we find the heat of formation of CH_2CF^+ to be 232.6 kcal/mole. This is in good accord with the value determined from process (9) in $C_2H_2F_2$ in which the same fragment ions is involved. From this we conclude again that the eliminated hydrogen stems from the CHF group of the molecule. The correspondence between the peaks in the yield curves of $C_2H_3F^+$ and $C_2H_2F^+$ at about 16.6 eV indicates that the same molecular states are initially being excited and then decay by autoionization followed by dissociation for those autoionized molecules having sufficient internal energy.

The bond rupture whereby CH_2CHF^+ loses a fluorine atom

$$C_2H_3F + h\nu \rightarrow C_2H_3^+ + F + e\,, \qquad (6)$$

gives, with $AP(C_2H_3^+) = 13.84 \pm 0.04$ eV, the heat of ormation of the vinyl ion $\Delta H_f(C_2H_3^+) = 271$ kcal/mole.

This value is 6 – 7 kcal/mole higher than that based on the formation of $C_2H_3^+$ in reactions (1) and (2); presumably we have to add a vibrational excess energy term in (6). There may also be an error in the literature with regard to $\Delta H_f(C_2H_3F)$ because other heats of formation quoted there are known to be not reliable. But we think it permissable to use this value nevertheless because of the consistency of the results in reactions (5) and (7). Taking our values of $AP(C_2H_3^+)$ and $IP(C_2H_3)$ we may compute $D(C_2H_3 - F)$ from the relation

$$D(C_2H_3 - F) = AP(C_2H_3^+) - I(C_2H_3)$$

to be less than 119 kcal/mole. This establishes the internal consistency of all data used as, on the

other hand, one may calculate, independent of $AP(C_2H_3^+)$ in (5),

$$D(C_2H_3-F) = +\Delta H_f(C_2H_3F) + \Delta H_f(C_2H_3) + \Delta H_f(F) = 111 \pm 3 \text{ kcal/mole};$$

the difference of the two dissociation energy values is of the same order of magnitude as that stated for $\Delta H_f(C_2H_3^+)$.

The ions C_2HF^+ and $C_2H_2^+$ have lower appearance potentials than the parent-minus-hydrogen respectively parent-minus-fluorine ions. Therefore they must be formed by a unimolecular direct H_2 or HF split from the parent:

$$C_2H_3F + h\nu \rightarrow C_2HF^+ + H_2 + e. \quad (7)$$

In the absence of internal rearrangement, the structure of the transition state then determines the structure of the resulting ion, $HCCF^+$ or $^{H}_{F}CC^+$, for which we calculate the heat of formation to be $\Delta H_f(C_2HF^+) = 288.4$ kcal/mole.

By use of the photoelectronspectroscopically determined $IP(CHCF) = 11.26$ eV [24] and $\Delta H_f(HCCF) = 25.5 \pm 2.5$ kcal/mole estimated from an electron impact study [25], one obtains $\Delta H_f(CHCF^+) = 285.2$ kcal/mole. The agreement of this and our value indicates that, unless there is merely fortuitous agreement, the fragmentation we observe produces the acetylene structure $HCCF^+$ and little if any excess energy is involved. This result, the loss of HCl from C_2H_3Cl (see above) and of H_2 from C_2H_4 examined by Botter et al. [26], provide some support for the assumption that processes involving the loss of a molecule do not always proceed over a potential barrier. The corresponding HF-elimination reaction

$$C_2H_3F + h\nu \rightarrow C_2H_2^+ + HF + e \quad (8)$$

involves only well known thermochemical data. Based on $AP(C_2H_2^+) = 13.51 \pm 0.02$ eV we calculate $\Delta H_f(C_2H_2^+) = 348.5$ kcal/mole, this value being considerably higher than the value 317.2 kcal/mole established in (3) and (4). From kinetic studies on the decomposition of vinylfluoride in a single-pulse shocktube. The difference of 31 kcal/mole can be taken as an upper limit of the activation energy for the HF-splitting from C_2H_3F. Analysis of the HF eliminiation reaction in $C_2H_2F_2$ results in a required excess energy of 26 kcal/mole, indicating the approximate validity of this result.

Ic. 1.1-Difluoroethylene

The onset of ionization is located at 10.29 ± 0.01 eV in good agreement with the adiabatic ionization potential $IP(CH_2CF_2) = 10.30$ eV found in Reference [17]. At higher energies we observe four simple bond rupture fragmentations, the first producing a fluorine atom by the process:

$$CH_2CF_2 + h\nu \rightarrow CH_2CF^+ + F + e. \quad (9)$$

The value of $\Delta H_f(CH_2CF_2) = -80 \pm 2$ kcal/mole was obtained by averaging the various values given in Reference [28]. Using this value the heat of formation of CH_2CF^+ was found to be $\Delta H_f(CH_2CF^+) = 235.3$ kcal/mole, in agreement with the value obtained from (5). We conclude that no excess energy is involved in both reactions.

Taking the process

$$CH_2CF_2 + h\nu \rightarrow CHCF_2^+ + H + e \quad (10)$$

we derive an upper limit for the heat of formation of $CHCF_2^+$, $\Delta H_f(CHCF_2^+) \leqq 496.5 \pm 2$ kcal/mole as it is not clear if we observed the true adiabatic threshold or not.

As is clearly seen from Fig. 5 the magnitude of initial rise in the $C_2H_2^+$ ion yield is approximately equal to the magnitude of the decrease in CH_2CF^+ intensity. We conclude that the overall reaction for this process can be written as

$$CH_2CF_2 + h\nu \rightarrow CH_2CF^+ + F + e \rightarrow C_2H_2^+ + 2F + e. \quad (11)$$

With the observed appearance potential $AP(C_2H_2^+) = 19.08$ eV, we obtain $\Delta H_f(C_2H_2^+) = 322.2$ kcal/mole which is 5 kcal/mole higher than the value derived from the photoionization of C_2H_2 [Equation (4)]. This difference may be due to the very slow rise in the threshold region. But one also could assume that in the fragmentation process $C_2H_2^+$ is formed in a state described by the geometry H_2CC^+ and not in the acetylenic structure $HCCH^+$. Calculations on the energetic difference of both species are intended. At 19.34 eV an increase in the ion efficiency curve of $C_2H_2^+$ is observed. This coincides with the begining of the fifth ionization potential of CH_2CF_2, the vertical transition of which is located at 19.68 eV [17].

A similar increase with different intensity can be seen in the CF^+, CH_2F^+ and CH_2^+ efficiency curves. This is explained by the higher internal excitation energy of the parent ion when ionization of a higher orbital is achieved. Correspondingly, the bonding properties within the molecular ion may be altered. Then a change of the reaction rates for the different fragmentations may occur. In a similar way one

may explain the strong rise in the CH_2CF^+ yield at the third ionization potential (15.73 eV) and the weak increase in the $CHCF_2^+$, CH_2CF^+ and CFH_2^+ efficiency curves in the neighbourhood of the energy of the fourth vertical ionization potential at 18.22 eV. In contrast to C_2H_3Cl and C_2H_3F, the C=C bond breaking process in CH_2CF_2 occurs with a rate sufficient to be detected and measured in our mass spectrometer:

$$CH_2CF_2 + h\nu \rightarrow CH_2^+ + CF_2 + e\,. \qquad (12)$$

The thermochemical data, $IP(CH_2) = 239.9$ kcal/mole [29] (which supposedly refers to the triplet ground state of CH_2) and $\Delta H_f(CH_2) = 92.1$ kcal/mole [16], are well established; added, they result in $\Delta H_f(CH_2^+) = 331.9$ kcal/mole. Equation (12) then yields $\Delta H_f(CF_2) = -20.1$ kcal/mole. This value lies within the wide limits, -5 to -45 kcal/mole, available in the literature [30]. Taking the electron impact ionization potential of the CF_2 radical to be 11.7 eV, Walter et al. [5] conclude $\Delta H_f(CF_2) = -43.4$ kcal/mole from the photoionization process

$$C_2F_4 + h\nu \rightarrow CF_2^+ + CF_2 + e\,. \qquad (13)$$

If we instead use our value for $\Delta H_f(CF_2)$ and the $AP(CF_2^+)$ from (13), we arrive at $IP(CF_2) = 9.74$ eV. The great discrepancy indicates that both the value for $IP(CF_2)$ and $\Delta H_f(CF_2)$ must be accepted with caution. However, one may conclude [30], by analogy with the stabilizing effect of F-atoms on the CH_2F^+, CHF_2^+ and CF_3^+ ions, that $IP(CF_2)$ is lower than $IP(CH_2) = 10.396$ eV [29]. We think therefore our value to be the more reliable one. The formation of CH_2^+ has to compete with fragmentation processes starting at lower energies. In this case the statistical theory of mass spectra [13] predicts a slowly rising efficiency curve with some curvature and vanishingly small ion intensities at energies appreciably above the theoretical appearance potential. Due to the low energy tail of the CH_2^+ efficiency curve we may not exclude this possibility. In terms of fragmentation following the transition to a steeply rising repulsive $CH_2CF_2^+$ state the high-energy shift of the CH_2^+ onset may be ascribed to kinetic energy of the fragments.

Reaction (12) applied to determine the dissociation energy of the C=C bond yields

$$D(CH_2=CF_2) = AP(CH_2^+) - IP(CH_2) \leqq 152 \text{ kcal/mole},$$

as compared to the electron impact value of 125 kcal/mole [32]. The great difference again indicates that the problem of an accurate determination of the C=C dissociation energy in ethylene and its derivatives by photodissociative ionization is not yet solved. Due to the formation of a molecule with a strong bond out of a unimolecular transition complex, the HF elimination process possesses the lowest appearance potential of all fragmentations in CH_2CF_2:

$$CH_2CF_2 + h\nu \rightarrow CHCF^+ + HF + e\,. \qquad (14)$$

With $AP(CHCF^+) = 14.18$ eV we obtain $\Delta H_f(CHCF^+) = 312$ kcal/mole which is in disagreement by 25 kcal/mole with the average value derived from C_2H_3F and CHCF (see above). This excess energy again is explained in terms of activation energy necessary to reach the transition state. However, we now get a value which is 6 kcal/mole lower than the one calculated from reaction (7).

One may point out that, whereas the structure of the ion resulting in process (8) may be $CC^{H^+}_H$ or $HCCH^+$, we are sure to get acetylenic $HCCF^+$ ions in (14). Taking it to be true that the excess energy of 5 kcal/mole in reaction (11) is due to the formation of the state CH_2^+, there is strong indication that the higher activation energy for HF elimination from C_2H_3F also refers to the formation of CCH_2^+.

The CF^+ and CH_2F^+ ions are assumed to be formed by the rearrangement processes

$$CH_2CF_2 + h\nu \rightarrow CF^+ + CH_2F + e \qquad (15)$$

and

$$CH_2CF_2 + h\nu \rightarrow CH_2F^+ + CF + e \qquad (16)$$

the similar feature of both ion yield curves indicates the common transition state which serves as a precursor of the fragmentation. With $\Delta H_f(CF) = 62$ kcal/mole [33] and (16) we get $\Delta H_f(CH_2F^+) = 200 \pm 3$ kcal/mole. By photoionization Walter et al. [5] determined the heat of formation of CF^+ to be about 275 ± 1 kcal/mole at room temperature. Taking (15) we arrive at $\Delta H_f(CH_2F) = -11$ kcal/mole. The $IP(CH_2F)$ may then be estabilished to be 9.16 ± 0.02 eV which is in resonable agreement with the electron impact value of 9.35 eV [34]. The difference of 0.08 eV between the appearance potentials of CF^+ and CFH_2^+ can be ascribed to the different ionization potentials according to

$$\begin{aligned} AP(CF^+) - AP(CFH_2^+) &= \Delta H_f(CF^+) + \Delta H_f(CFH_2) \\ &\quad - \Delta H_f(CH_2F^+) - \Delta H_f(CF) \\ &= IP(CF) - IP(CH_2F)\,. \end{aligned}$$

We get $IP(CF) = 9.24$ eV in good agreement with the value 9.23 eV determined by photodissociative ionization of C_2F_4 [5].

II. Parent Ion Efficiency Curves

In the following we will discuss the structure in the photoionization efficiency curves of C_2H_3Cl, C_2H_3F and $C_2H_2F_2$ in terms of vibrational and electronic excitation of the ion as well as autoionization from neutral excited states.

The threshold law for direct photoionization is known to be approximately a step function [31], each step indicating the existence of an isolated electronic state of the parent ion. Excited states of that kind are observed only if the internal energy of the ion is insufficient to decompose the ion or the fragmentation takes a longer time than the 10^{-6} seconds characteristic for the entering of the ions into the mass spectrometer. In Fig. 7 and 8 the onset region of $C_2H_3F^+$ and $C_2H_2F_2^+$ is given. A comparison with the vibrational fine structure in the photoelectron spectrum [17] clearly indicates the steps to be transitions into vibrational excited states of the ions. The first step corresponds to the adiabatic ionization potential of a $\pi(C=C)$ electron in each case, In correspondence with the photoelectron spectrum, the $CH_2CF_2^+$ efficiency curve exhibits all excited levels of the C=C stretching vibration. Where we found $\nu(C=C) = 1535\ cm^{-1}$, the vibrational structure in the photoelectron spectrum gives $1605\ cm^{-1}$.

Ionization of C_2H_3Cl at 11.65 eV does not coincide with fragmentation processes in contrast to ionization out of higher orbitals in C_2H_3F and CH_2CF_2. Correspondingly, this first excited ion state of vinylchloride is the only one to be identified as a step in the $C_2H_3Cl^+$ efficiency curve. Similar steps are not seen beyond the onset region in the $C_2H_3F^+$ and $CH_2CF_2^+$ efficiency curves.

Figures 3 – 5 present a different type of structure, rather pronounced peaks which have to be identified as neutral excited states which autoionize and distort the photoionization cross section.

This kind of structure is well known for diatomic and small organic molecules (e. g. H_2CO [34]) and can be understood in terms of autoionizing Rydberg states converging to higher ionization potentials. Our results give clear evidence of this mechanism only in the case of vinylchloride, as in shown in Fig. 6 in detail. A comparison of the parent ion efficiency curves indicates that autoionization involving rather broad molecular bands dominates as was also found for other molecules [4, 5]. This prevents additionally the observation of any steplike behaviour. Those Rydberg states of C_2H_3Cl lying in front of the LiF edge were also detected by Sood and Watanabe [9] but could not be assigned. Using the step at 11.65 eV as the Cl-3p ionization potential, we ordered this series according to the Rydberg formula:

$$\nu = IP - R/(n-\delta)^2.$$

The quantum defect δ was determined by averaging the δ-values of the observed series. Table 2 gives the frequencies of the measured transitions according to their quantum defect associated with *n*s, *n*p and *n*d series. We are not able to reproduce the sharp autoionization peaks Momigny observed in C_2H_3Cl and fluorinated ethylenes [6]; this discrepancy may be due to our better experimental conditions (higher resolution, continuum light source).

Table 2. Rydberg series in the photoionization spectrum of vinylchloride (energies in eV).

	n s	*n* p	*n* d
δ	0.82	0.48	0.17
n		10.54	10.72
4	10.28	10.98	11.05
5	10.86	11.20	11.25
6	11.15	11.35	11.36
7	11.29		11.43
8			
∞		11.65	

In their photoelectron spectrum, Lake and Thompson assigned two vertical ionization potentials at 11.72 and 11.87 eV as originating from the Cl(3p) a′ and a″ electrons [17]. Our results tend to confirm the assumption of Klasson and Manne [36] that the two close-lying states belong to the same electronic state. They calculated the chlorine 3p lone-pairs, one in the plane of the molecule (a′ or π') and one perpendicular to this plane (a″ or π), to be separated by about 1.3 eV. We then associate the step to be seen in the ionization efficiency curve with the 3p(a′) orbital. This assignment agrees with the photoelectron spectrum of Robin et al. [37] who located the 3p ionization at 11.66 eV. Corresponding Rydberg series converging to the fluorine 2p orbitals lying at 17.4 eV in the atom were not detected, perhaps for the following reason. The fluorine 2p orbitals are lying to a greater extent than the

chlorine 3p-orbitals within the molecular framework, therefore often participating extensively in the σ-bonding of the molecule [38]. Excited states may then be described as broad valence shell states rather than as Rydberg states. Provided the latter states exist, an interaction of the superexcited and the autoionized orbital which is too weak would prevent the occurence of resonance structure in the ionization efficiency curve. An example of a low autoionization probability was presumably found by Chupka et al, [18] concerning Rydberg-series converging to the first excited state of the ethylene ion.

As a further explanation, one may suggest a severe broadening of sharp structure due to fast predissociative processes, i. e. lifetimes being at least of the order 10^{-13} sec.

Then neither the parent ion nor the resulting fragmentation efficiency curve would give clear indication of sharp absorption. As stated above the origin of broad bands is thought to be due in most cases to transitions from higher electronic orbitals to the first vacant orbitals of π^* or σ^* type. We therefore tried to combine the energetic position of these transitions with the aid of the known orbital energies [17] and the $\pi^* \leftarrow \pi$ transitions to be found in the ultraviolet [38, 39] according to

$$E = \Delta E + (\pi^* \leftarrow \pi),$$
$$\Delta E = I(\pi\text{-orbital}) - I(\text{higher orbital}).$$

The $\pi^* \leftarrow \pi$ transition energies were taken to be 6.7 eV (C_2H_3Cl) [39], 7.44 eV (C_2H_3F) and 7.5 eV (CH_2CF_2) [38]. All symmetry- allowed transitions of interest are summarized in Table 3 together with the ionization potentials measured by Lake and Thompson.

As it is impossible to take the various Franck-Condon factors into account when joining the different energies, the reliability of E and ΔE determined in this way may not be very good. Although some agreement is seen in all spectra, the most prominent band in CH_2CF_2, occuring near 14 eV, cannot be explained. For all compounds the structured region is followed by a slow decrease of the photoionization cross section starting at about 20 eV. As was observed in the absorption spectrum of other hydrocarbons [12, 40], the total absorption cross section decreases beyond the valence shell region too.

Table 3. Ionization potentials determined by photoelectron spectroscopy [17] and calculated transition energies in the VUV.

	IP (eV) vertical	*IP* (eV) adiabatic	$\Delta E + (\pi^* \leftarrow \pi)$
C_2H_3Cl	10.18	10.00	
	11.72		
	11.87		
	13.14		
	13.56		
	15.39		12.09
	16.31		13.01
	18.76		15.46
C_2H_3F	10.58	10.37	
	13.79		
	14.51		11.58
	16.77		13.84
	17.97		15.04
$C_2H_2F_2$	10.72	10.31	
	14.79	14.06	
	15.73		
	18.22		
	19.68		

Acknowledgements

We thank Prof. H. Zimmermann, Freiburg i. Br., and Prof. R. Haensel, Hamburg, who enabled us to do this work. Financial support of the Deutsche Forschungsgemeinschaft and the Deutsches Elektronen-Synchrotron DESY is gratefully acknowledged.

[1] K. Siegbahn et al., ESCA Applied to Free Molecules, North Holland, Amsterdam 1969.
[2] D. W. Turner, C. Baker, A. D. Baker, and C. R. Brundle, Molecular Photoelectron Spectroscopy, Wiley and Sons, London 1970.
[3] V. H. Dibeler and R. M. Reese, J. Res. Nat. Bur., Stand. **68 A**, 409 [1964].
[4] W. A. Chupka and J. Berkowitz, J. Chem. Phys. **47**, 2921 [1967].
[5] T. A. Walter, C. Lifshitz, W. A. Chupka, and J. Berkowitz, J. Chem. Phys. **51**, 3531 [1969].
[6] J. Momigny, Thèse d'Agrégation de l'Enseignement supérieur, Université de Liège (1966).
[7] C. Lifshitz and F. A. Long, J. Phys. Chem. **67**, 2463 [1963].
[8] C. Lifshitz and F. A. Long, J. Phys. Chem. **69**, 3731 [1965].
[9] S. P. Sood and K. Watanabe, J. Chem. Phys. **45**, 2913 [1966].
[10] R. Haensel and C. Kunz, Z. Angew. Physik **23**, 276 [1967].
[11] M. Skibowski and W. Steinmann, J. Opt. Soc. Amer. **57**, 112 [1967].
[12] E. E. Koch and M. Skibowski, Chem. Phys. Letters **9**, 429 [1971].
[13] J. A. R. Samson, Techniques of Vacuum Ultraviolet Spectroscopy, Wiley and Sons, New York 1967, and references given therein.
[14] D. Reinke, Thesis, Universität Freiburg i. Br. (in preparation).
[15] R. Kraessig, Thesis, Universität Freiburg i. Br. (in preparation).
[16] JANAF Thermochemical tables, 2nd Ed. (Washington, Nat. Bur. Stand. NSRDS-NBS 37, 1971).

[17] R. F. Lake and Sir H. Thompson, Proc. Roy. Soc. London **A 315**, 323 [1970].
[18] W. A. Chupka, J. Berkowitz, and K. M. A. Rafaey, J. Chem. Phys. **50**, 1938 [1969].
[19] A. M. Joshi and B. J. Zwolinski, Polym. Letters **3**, 779 [1965].
[20] D. Beck, Dis. Faraday Soc. **36**, 56 [1963].
[21] J. A. Kerr, Chem. Rev. **66**, 465 [1966].
[22] J. Omura, T. Kaneko, and Y. Yamada, J. Phys. Soc. Japan **27**, 178 [1969].
[23] P. G. Maslov and Y. P. Maslov, Klim. i. Technol. Popliva i Masel **3**, 50 [1958], and Chem. Abstr. **53**, 1910 [1959].
[24] H. J. Hainck, E. Heilbronner, V. Hornung, and E. K. Jensen, Helv. Chim. Acta **53**, 1073 [1970].
[25] E. K. Jensen, C. Pascual, and J. Vogt, Helv. Chim. Acta **53**, 2109 [1970].
[26] R. Botter, V. H. Dibeler, J. A. Walker, and H. M. Rosenstock, J. Chem. Phys. **45**, 1298 [1966].
[27] J. M. Simmie, W. J. Quiring, and E. Tschuikow-Roux, J. Phys. Chem. **74**, 992 [1970].
[28] J. M. Simmie and E. Tschuikow-Roux, J. Phys. Chem. **74**, 4075 [1970] and references given in that paper.
[29] G. Herzberg, Proc. Roy. Soc. London **A 262**, 291 [1961].
[30] R. Sisher, J. B. Homer, and F. P. Lossing, J. Amer. Chem. Soc. **87**, 957 [1965].
[31] W. A. Chupka, J. Chem. Phys. **30**, 191 [1959] and references given in that paper.
[32] J. S. Shapiro and F. P. Lossing, J. Phys. Chem. **72**, 5 [1968].
[33] T. L. Porter, D. E. Mann, and N. Acquista, J. Mol. Spectr. **16**, 228 [1965].
[34] F. P. Lossing, P. Kebarle, and J. B. Desousa, Advances in Mass Spectrometry, J. O. Waldron, Ed., Pergamon Press Ltd., London 1958.
[35] J. E. Mentall, E. P. Gentieu, M. Krauss, and D. Neumann, J. Chem. Phys. **55**, 5471 [1971]; P. Warneck, Z. Naturforsch. **26 a**, 2047 [1971].
[36] M. Klasson and R. Manne, in Electron Spectroscopy, Ed. D. A. Shirley, North Holland Publ. Comp., 6972, p. 471.
[37] M. B. Robin, N. A. Kuebler, and C. R. Brundle, ibid. [36], p. 351.
[38] G. Bélanger and C. Sandorfy, J. Chem. Phys. **55**, 2055 [1971].
[39] A. D. Walsh, Trans. Faraday Soc. **41**, 35 [1945].
[40] E. E. Koch, Absorption Spectrum of Ethylene, unpublished results.

Reaktivitätsabschätzungen an substituierten Phenolen mit Hilfe semiempirischer MO-Methoden. II.

H. Sterk und W. Hopels

Institut für Organische Chemie der Universität Graz

(Z. Naturforsch. **28 a**, 1031–1035 [1973]; eingegangen am 31. Januar 1973)

Estimations of Reactivity on Substituted Phenols by Semiempirical MO-methods

An attempt is made, to investigate the reactivity of aromatic compounds by a stepwise approach of the NO_2-cation to the aromatic system, by means of the MINDO-II method.

Die Nitrierung bzw. Diazotierung verläuft in Bezug auf das Substrat in der Regel nach demselben Mechanismus. Zwar kann das angreifende Teilchen auf verschiedenartigste Weise gebildet werden, der Einfluß auf die π-Elektronen am Aromaten – in Form einer Ladungsdelokalisierung des Aromaten – bleibt jedoch qualitativ immer derselbe. Wir wissen heute, daß aromatische Moleküle Additionsverbindungen einzugehen vermögen [1–4], die entweder von der Art der π-Komplexe sind, wobei das Elektrophil auf Grund des π-Sextetts an den Aromaten gebunden ist, oder von der Art der als Carboniumionen formulierten, aber meist als σ-Komplexe bezeichneten Übergangszustände. Bei den Versuchen, die Reaktionen am Aromaten mit Hilfe von MO-Daten zu interpretieren, wird daher die Frage aufgeworfen, inwieweit solche Übergangszustände verifiziert bzw. Attacken am System an Hand von Hyperflächen beschrieben und die, für den Reaktionsablauf maßgeblichen sterischen Gesichtspunkte, erfaßt werden können (vgl. [5–14]).

Um den Reaktionsablauf beim hier interessierenden System Phenol/NO_2^+ zu beschreiben, ist zunächst auf der Basis der Bildungsenthalpie des Gesamtsystems eine Energiehyperfläche erstellt worden, die ein Abbild der energetischen Situation zu Beginn der Reaktion wiedergeben soll. Energiewerte, die den Positionen der Nitrogruppe, in 3 Å Abstand von der Phenolebene, entsprechen – wobei die Ebene der Nitrogruppe senkrecht auf der Phenolebene steht – sind in Abb. 1 gezeigt.

Das Minimum befindet sich am para-C-Atom, während über den C – C-Bindungen Orte höherer Energie liegen und somit eine geringere Aufenthaltswahrscheinlichkeit für den Angreifer ergeben. Außerdem ist der Energieanstieg vom Minimum nach außen, zum p-H-Atom, bedeutend flacher, als in

Sonderdruckanforderungen an Doz. Dr. Heinz Sterk, Institut für Organische Chemie, Universität Graz, Heinrichstraße 28, *A-8010 Graz*, Österreich.